International Journal of Plasticity xxx (2013) xxx–xxx

Contents lists available at SciVerse ScienceDirect

International Journal of Plasticity

journal homepage: www.elsevier.com/locate/ijplas

Molecular dynamics simulations of compressive yielding in cross-linked epoxies in the context of Argon theory

V. Sundararaghavan *, A. Kumar

Aerospace Engineering, 3025 FXB building, 1320 Beal Ave, University of Michigan, Ann Arbor, MI 48109, USA

ARTICLE INFO

Article history:
Received 15 February 2012
Received in final revised form 25 December 2012
Available online xxxx

Keywords:
A. Yield condition
B. Polymeric material
C. Molecular dynamics

ABSTRACT

Molecular dynamics simulations are performed to study compressive yielding behavior of epoxy-amine cross-linked polymer networks in the low temperature glassy state. The simulations show a sharp drop in stresses after the elastic regime which was identified to occur due to the activation of wedge disclinations. For the first time in literature, both the chemistry and geometry (critical segment length, angles, bond torsions) involved in the molecular mechanism of compressive yielding have been measured. We analyze these results in the context of the Argon theory which is based on a linear elastic model of wedge disclination. The kink distance calculated using this simple theory gives a surprisingly good match to the results seen from the complex molecular simulation. The yield stress versus temperature predictions of Argon theory are directly compared with molecular simulation results. Finally, the use of Argon theory for extracting yield stresses at quasi-static strain rates from high rate molecular simulations is investigated.

© 2013 Elsevier Ltd. All rights reserved.

1. Introduction

Properties of Epoxy-based thermoset polymers can be tuned towards a variety of applications from stiff binders in fibers for aircraft structures to loose gels for biological membranes. Investigation of the physical origin of such versatile properties is of value in developing polymer networks with multifunctional properties such as superior energy dissipation, impact resistance and adhesion. Glassy epoxies undergo a well-defined yielding behavior under compressive loading. The observed Arrhenius form of exponential temperature dependence of the deformation rate at constant stress prompted early theoreticians to employ viscous flow theory of Eyring (1936). In Eyring's theory, yielding occurs by coordinated flow of molecular segments under the application of stress. However, the theory failed to predict the observed dependence of yield stress with temperature. The theory of Robertson (1966) had many similarities with the theory of Eyring. Robertson also proposed that the yield mechanism was due to increased fluidity under applied stresses although the particular mechanism employed was the conversion of molecules at low energy trans state to a high energy cis state. The model accounted well for the temperature dependence of yield stress around the glass transition temperature but failed at lower temperatures.

Subsequently, attempts were made to understand yield behavior in polymers using ideas from crystal plasticity approaches in metals. Li and Gilman (1970) and Gilman (1968) postulated that deformation occurs by localized coordinated slip rather than by homogeneous shear as in viscous flow theories. In particular, Gilman identified defects in glassy materials in the form of dislocations (involving partial chain displacement) and disclinations (involving chain twisting and kinking). Two separate theories were derived from these ideas: Bowden theory (Bowden and Raha, 1974) and Argon theory (Argon, 1975; Argon, 1973; Argon and Bessonov, 1977), relying on yielding driven by dislocations and disclinations, respectively.

* Corresponding author. Tel.: +1 734 615 7242.
E-mail address: veeras@umich.edu (V. Sundararaghavan).

0749-6419/$ - see front matter © 2013 Elsevier Ltd. All rights reserved.
http://dx.doi.org/10.1016/j.ijplas.2013.01.004

Please cite this article in press as: Sundararaghavan, V., Kumar, A. Molecular dynamics simulations of compressive yielding in cross-linked epoxies in the context of Argon theory. Int. J. Plasticity (2013), http://dx.doi.org/10.1016/j.ijplas.2013.01.004

Bowden's theory assumed that yielding starts as a shear patch made by a continuous distribution of dislocations. This model accounted well for the temperature and strain rate dependence of the yield stress closer to glass transition but did not satisfactorily predict yield stress at lower temperatures. Argon noted that disclinations play a larger role in yielding of amorphous polymers. Of the two types of disclinations (chain twisting and chain kinking) proposed by Li and Gilman (1970), Argon chose kinking disclination to be the activating mechanism for yielding. Argon theory performs best at low temperature glassy conditions and has been used to successfully interpret the yield behavior of a large number of epoxy thermosets in Refs. Lee (1988), Yamini and Young (1980) and Cook et al. (1998).

A concise review of molecular theories of plastic deformation in amorphous polymers can be found in Stachurski (1997). During the derivation of these theories, researchers did not have the tools needed to measure or simulate behavior at molecular length scales. With the advent of molecular models and accurate interatomic potentials, it may now be possible to directly visualize molecular mechanisms of yielding. In the case of metallic (crystalline) materials, molecular simulations have allowed detailed study of defect (dislocation) nucleation (Spearot et al., 2007; Kang and Cai, 2010) or structure (Weinberger, 2011; Xu et al., in press). Unlike crystalline metals, epoxies have an amorphous structure and the process of building such complex cross-linked molecular configurations with realistic properties is challenging and is being currently addressed by several researchers (see review in Knox et al. (2010)). In addition, molecular dynamics involve high strain rates ($> 10^6/s$) that are seldom seen in many industrial applications. In order to reconcile molecular dynamics results with real experiments, it is important to study strain-rate scaling laws. Of particular interest in this work is the yield behavior at low temperatures where Argon theory has been the most successful. Argon theory proposes a highly localized yielding mechanism that can be tested using MD simulations. In this work, For the first time in literature, molecular dynamics has been used to visualize the yielding mechanisms in cross-linked epoxies and to interpret the molecular parameters involved in Argon theory. Results from Argon theory are then compared with the yield-stress versus temperature predictions obtained from molecular simulations. The utility of Argon theory for extracting the yield stress at quasi-static strain rates from high rate molecular simulations is also investigated. The yield stress obtained from molecular dynamics is then compared to the experimentally measured yield stress (Heinz and Wiggins, 2010) (at quasi-static conditions) recently reported in literature.

2. Technical approach

For this study, a common epoxy was employed: Di-Glycidyl Ether of Bisphenol A (DGEBA). The epoxy and amine monomer structures are shown in Fig. 1. The epoxy molecules were cross-linked (cured) with $4-4'$ diamino diphenyl sulfone (DDS). Each epoxy monomer has two epoxide (oxirane ring) groups, each with a cross-linking functionality of one towards amine curing agents, for a total functionality of two; each DDS monomer has two amine groups, each with a functionality of two towards epoxy molecules, for a total functionality of four. The typical synthetic epoxy to amine stoichiometric ratio is approximately 2:1 or 33.3 mol% amine. Fig. 2 shows polymer formation driven by the bonding of epoxide group in DGEBA and the amine groups in DDS. During formation of a cross-link, the primary amine group reacts with epoxide group forming a bond between nitrogen of DDS and the terminal carbon of the epoxide group. The carbon–oxygen bond breaks between the terminal carbon and the epoxide oxygen forming an alcohol (-OH) link. The cross-linked structure in Fig. 2(a) can undergo further reaction with another epoxy molecule forming a cross-linked molecular structure (Fig. 2(b)). Epoxies used in industrial prepegs show an actual conversion between 70–95% when measured through Near-Infrared (NIR) Spectroscopy (Wang et al., 2003). The conversion percentage depends on the process conditions, most importantly, the temperature and time of curing.

Many approaches have been recently used to build cross-linked polymer network systems with more than 70% conversion rate for use in molecular dynamics simulations. Most of these approaches involve polymerizing unreacted monomer mixtures over time (multi-step) or all-at-once (one-step). In one-step cross-linking (Yarovsky and Evans, 2002; Rottach et al., 2007), sites are randomly selected and pairs of sites within a capture radius are cross-linked together. One-step methods lead to artificially high network strains. In multi-step cross linking (Heine et al., 2004; Varshney et al., 2008; Wu and Xu, 2006) all reactive pairs that satisfy a given length criteria are cross-linked. The length criteria increases with each iteration and equilibration and cross-linking are repeated until desired cross-linking density is reached. Although multi-step methods prevent and relieve network strains, these are computationally intensive. Christensen (2007) introduced a new method to

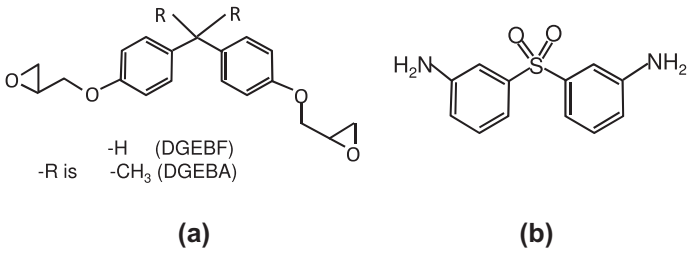

Fig. 1. Chemical structure of epoxy resin. DGEBA and the amine monomer diamino diphenyl sulfone employed in this work.

Please cite this article in press as: Sundararaghavan, V., Kumar, A. Molecular dynamics simulations of compressive yielding in cross-linked epoxies in the context of Argon theory. Int. J. Plasticity (2013), http://dx.doi.org/10.1016/j.ijplas.2013.01.004

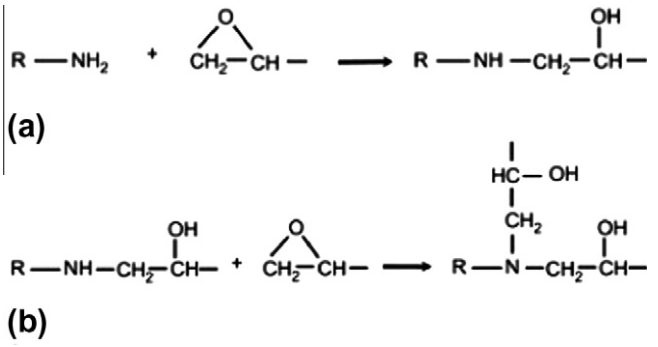

Fig. 2. Epoxy-amine cross linking through reaction of amine group with epoxide group.

build epoxy networks using a 'dendrimer' growth approach. In this approach, the thermoset resin is modeled by starting with a single monomer and then cross-linking a second layer of monomers around it. In the next step, a third layer of monomers are cross-linked to the second layer. In this way, generations (layers) of monomers are added to a seed structure that grows in size at every pass. The principal advantages of the dendrimer growth method are the complete avoidance of artificial network strain during curing and the low computational cost of the growing procedure. Monomers can be manually added to the outermost generation to cross-link unreacted pairs of sites and increase cross-link density.

Materials Studio software (Accelrys Software Inc, 2007) was used to build a dendrimeric structure with 36 amine groups and 71 epoxy groups resulting in a total of 4601 atoms. In the initial dendrimer (see Fig. 3), 75% of available epoxy sites were cross-linked which is representative of many structural epoxies (Wang et al., 2003). Use of a small 4601 atom system was motivated by the fact that all simulations in this work are performed under periodic boundary conditions and the representative epoxy structure provided sufficient complexity needed to capture the amorphous nature of the polymer. The correctness of the representation was further studied (i) by comparing the dilatometric curve predicted by MD with experimental result and (ii) by testing if the structure is isotropic using the full anisotropic elastic stiffness matrix computed from molecular statics. For all simulations presented in this study, CVFF (Consistent Valance Force Field) potential (Dauber-Osguthorpe et al., 1988) was used for bonded as well as non-bonded interactions. This force-field successfully predicted accurate thermodynamic properties of interest for epoxies in a previous study (Varshney et al., 2008).

To model the equilibrated structure, the initial dendrimer structure was first optimized by minimizing the energy of the structure using 10000 iterations of a conjugate gradient (CG) minimizer. Subsequently, molecular dynamics was performed over several annealing cycles. Each annealing cycle involved a NPT (isothermal–isobaric ensemble) simulation at very low temperature (1 K) followed by another NPT run at 600 K (which is above glass transition temperature $T_g \approx 425 - 495$ K for DGEBA/DDS (Tcharkhtchi et al., 2000). These simulations were performed at 1 atm pressure for 10000 steps each (at

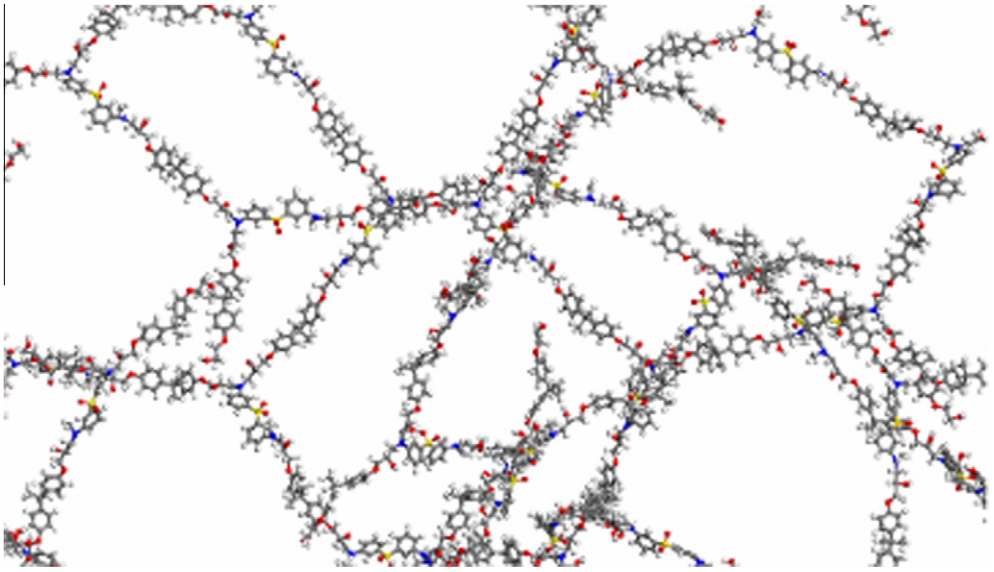

Fig. 3. 3D dendrimer used to build the molecular model of a cross-linked epoxy structure.

Please cite this article in press as: Sundararaghavan, V., Kumar, A. Molecular dynamics simulations of compressive yielding in cross-linked epoxies in the context of Argon theory. Int. J. Plasticity (2013), http://dx.doi.org/10.1016/j.ijplas.2013.01.004

1 fs time step). The density was tracked over successive anneal cycles until convergence was seen. A final density of 1.17 g/cc at 1 K and 1 atm pressure was obtained.

Further mechanical tests were performed in the LAMMPS package (Plimpton, 1995) that has methods for imposing realistic boundary conditions. The dendrimer structure in Materials Studio was exported to LAMMPS using the same CVFF potential. A sufficiently large atom-based Lennard–Jones/Coulomb interaction cutoff of 12.5 Å was used in the process. In LAMMPS, the system was subject to NPT simulations at various temperatures to compute the thermal expansion coefficient. The change in cell length with temperature is superposed with experimentally measured dilatometric curve reported in Tcharkhtchi et al. (2000) in Fig. 4 and the data shows good agreement. The linear coefficient of thermal expansion between 223 K to 323 K is measured to be 54.6 μ/K from this figure.

The elastic stiffness tensor of the optimized epoxy structure was then calculated. Computation of elastic properties involved 12 (molecular statics based) mechanical tests (Theodorou and Suter, 1986). These include three tension tests and three compression tests (along x, y and z direction respectively with zero lateral contraction) and six shear tests (xy, yz, xz shear; in both positive and negative directions). The strain increment is taken to be reasonably small (0.001) and CG minimization for 10000 steps is carried out to get equilibrated atomic positions at this strain. In effect, the calculation corresponds to a temperature of 0 K and static loading. The Young's modulus and Poisson's ratio of the epoxy structure are computed as a function of in-plane (x–y plane) loading direction (by rotating the calculated stiffness matrix) and the variation is shown in Fig. 5. It can be seen that the system has close to isotropic properties with a mean elastic modulus of 4.83 GPa and a Poisson's ratio of 0.33. Elastic modulus decreases with increase in temperature. At room temperature (300 K) and quasi-static loading rates, a peak elastic modulus of 3.76 GPa and a Poisson's ratio of 0.37 have been measured in experiments (Heinz and Wiggins, 2010).

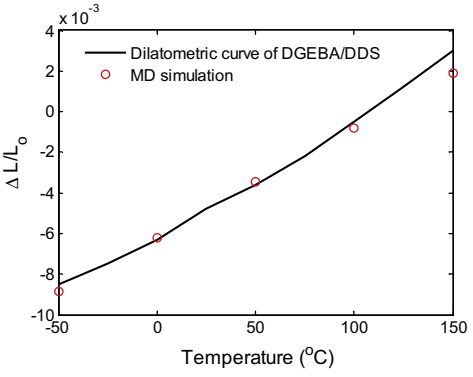

Fig. 4. The thermal expansion behavior computed using MD calculations are superposed with experimentally measured dilatometric curves reported in Tcharkhtchi et al. (2000).

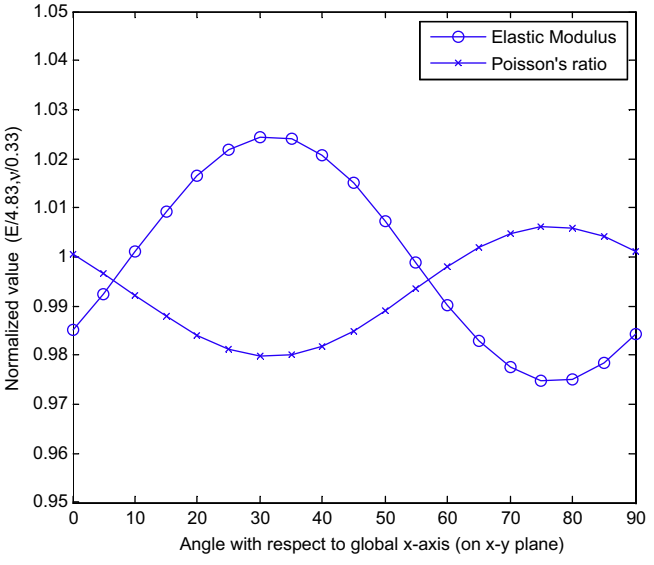

Fig. 5. Variation of elastic properties along various directions in the x–y plane. The results show an almost isotropic response.

Please cite this article in press as: Sundararaghavan, V., Kumar, A. Molecular dynamics simulations of compressive yielding in cross-linked epoxies in the context of Argon theory. Int. J. Plasticity (2013), http://dx.doi.org/10.1016/j.ijplas.2013.01.004

Subsequently, compression tests were performed on the periodic cell. The strain along x-direction was controlled by adjusting the periodic boundary conditions over time at a specified strain rate. The lateral boundaries follow both periodicity (in the y- and z- directions) and traction-free boundary conditions. To realize traction-free boundary conditions, barostats were used to adjust the pressure along y- and z- directions to 1 atm ambient pressure. Note that the y- and z- pressures were enforced independently (and not coupled together; allowing for anisotropic response). These boundary conditions enable realistic simulation of a compression test. Engineering strain rates were specified along x-direction stepwise in time. In between the strain steps, the system is equilibrated for 1 ps (1000 timesteps). Running time averages over the last 0.5 ps of the equilibration step were used to compute stress at that particular strain value. The resulting stress tensor computed is the negative of the internal pressure tensor, which includes both kinetic energy and virial terms (Frenkel and Smit, 2002). Velocity imposed in the system was about 38 m/s for 10^{10} s^{-1} strain rate test which is considerably lower than speed of sound in the solid which is 1834 m/s at 1 K.

3. Results

The results of the 10^{10} s^{-1} strain rate test were used to extract the elastic modulus (E), Poisson's ratio (ν) and yield stress at different temperatures (T). The elastic properties were extracted by fitting stress–strain data up to a strain of 0.05. The elastic modulus is seen to decrease with increase in temperature as shown in Fig. 6(a) with $E(T) = 8.38 - 0.012T$ linear fit. Poisson's ratio does not show a strong dependence on temperature with a best fit of $\nu = -0.0001092T + 0.361$ as shown in Fig. 6(b). The elastic modulus increases with increase in strain rate. For example, MD result at the 10^{10} s^{-1} strain rate is 7.62 GPa at 1 K compared to 4.83 GPa computed from molecular statics simulation. Poisson's ratio does not change significantly with strain rate, with a value of 0.33 computed from molecular statics as compared to 0.349 computed at a strain rate of 10^{10} s^{-1}. The representative results of the compression tests in the form of stress–strain response at T = 1 K, 112 K and 301 K are shown in Fig. 7(a). The stress increases initially with strain (in the elastic and anelastic regime) until it reaches a maximum value (at around 10% strain). Subsequently, a steep drop in stress is observed (which is related to the initiation of a molecular defect and is studied later in this paper). As deformation proceeds beyond this point, the stress increases again until another chain defect nucleates and a second steep drop in stress is seen. The defect mechanisms are better visualized in the context of a smaller polymer system considered here. When using a large polymer system, the defect generation process is continuous due to the availability of a larger number of chains where defects can nucleate, and as a result the stress–strain profile is smoother (Jaramillo et al., 2012). The stress value and the corresponding strain at the start of the first steep drop in stress are taken to be the yield stress and yield strain respectively. The variation of yield stress with temperature is shown in Fig. 7(b).

In thermoset epoxies, experiments reveal an Arrhenius form of exponential temperature (T) dependence of the strain rate ($\dot{\gamma}$) at constant stress:

$$\dot{\gamma} = \dot{\gamma}_o \exp\left(-\frac{\Delta G^*}{k_b T}\right) \tag{1}$$

Here, $\dot{\gamma}_o$ is a pre-exponential factor (taken to be 10^{13} s^{-1} (Lee, 1988)), k_b is the Boltzmann constant and ΔG^* is the critical free energy of activation of the molecular mechanism of yielding. In the theory proposed by Argon (1975), a molecular mechanism of yielding by formation of a pair of molecular kinks is considered. The local deformation process is shown in Fig. 8(a) in

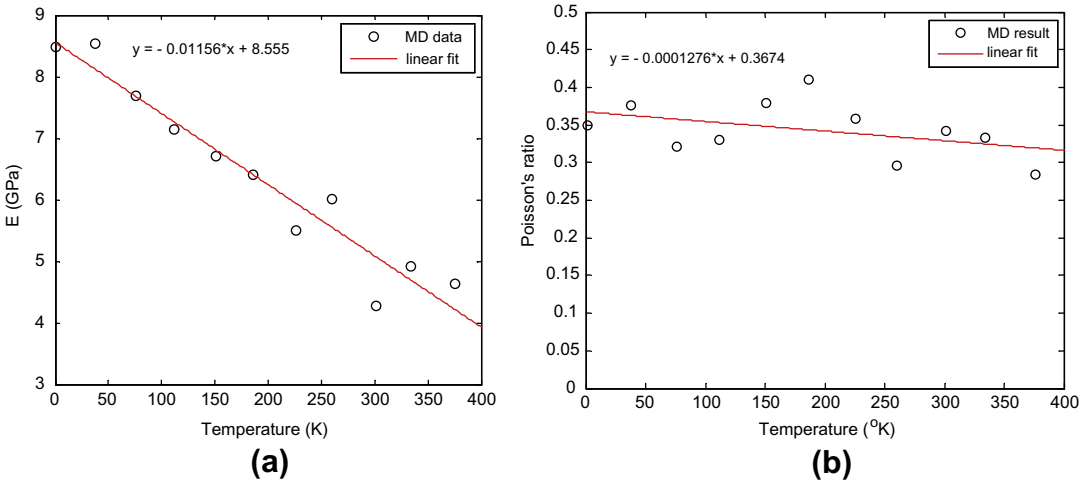

Fig. 6. Variation of (a) Elastic Modulus and (b) Poisson's ratio with temperature as measured from MD calculations at a strain rate of 10^{10} s^{-1}.

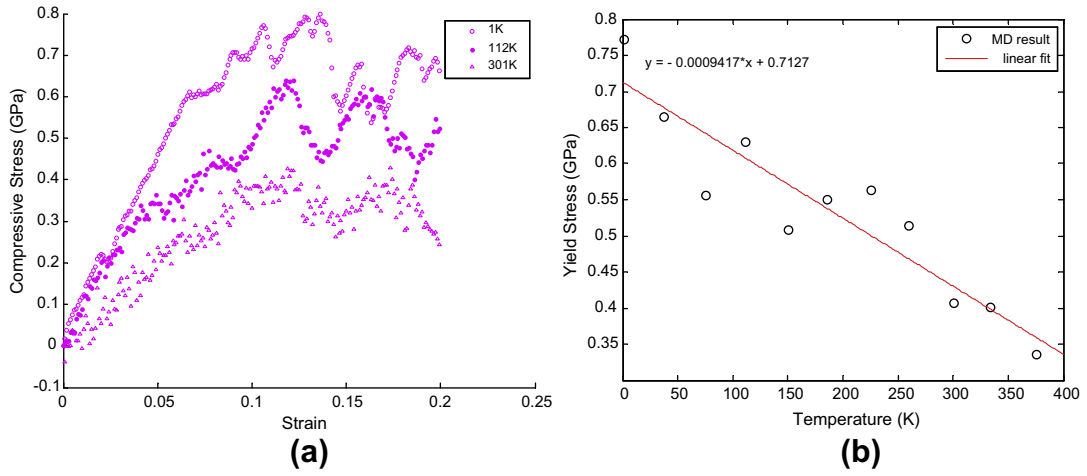

Fig. 7. (a) Compressive stress–strain response at three different temperatures as measured from MD simulations. (b) Variation of yield stress with temperature as measured from MD simulations at a strain rate of $10^{10}\ s^{-1}$.

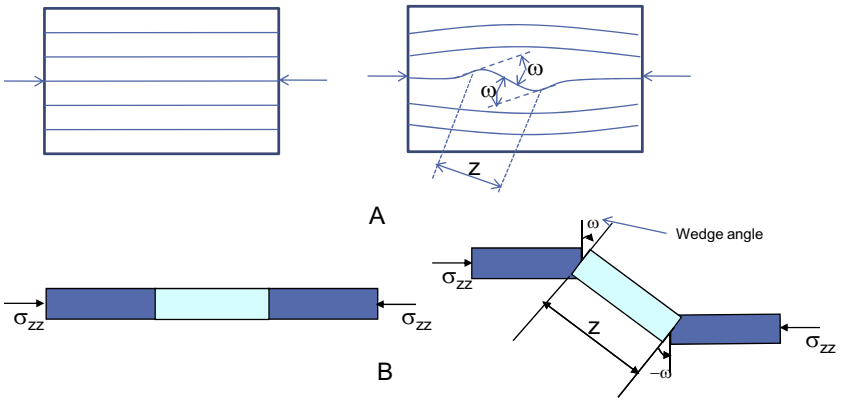

Fig. 8. (a) The work of Argon (Argon, 1975) postulates that yielding under compression is related to activation of a double kink in a flexible molecular segment. (b) The double kink is modeled as a wedge disclination dipole, with wedge angle of ω and critical segment length of z.

which a flexible chain kinks by rotating an angle ω at two centers of rotation located a distance z apart. The displacement field of the kink can be found by modeling two wedge disclination loops extending over the molecular diameter ($d = 2r$) and located at the two centers of rotation.[1] The elastic displacement and stress field of a double wedge disclination was first solved by Li and Gilman (1970). The surrounding molecules that oppose kink formation were modeled as an elastic continuum with bulk isotropic properties of the epoxy structure. Using this approach, the change in free enthalpy of the polymer due to creation of a single double wedge disclination can be obtained as:

$$\Delta G = \frac{3\pi\mu\omega^2 r^3}{16(1-\nu)} - \frac{9\pi\mu\omega^2 r^3}{8(1-\nu)}\left(\frac{r}{z}\right)^5 - \pi\mu\omega^2 r^3 \frac{\tau}{\mu}\frac{z}{r} \tag{2}$$

Here, ν is the Poisson's ratio and $\mu = \frac{E}{2(1+\nu)}$ is the shear modulus. The first term gives the self-energies of the two kinks and the second term gives the interaction energy of the kinks and are taken from the work of Li and Gilman (1970). The third term gives the work done by the external stresses during production of the pair of kinks. To obtain this term, the strain produced by a double kink along the z-direction is found by scaling the strain of the double kink $(1 - \cos(\omega))$ with the volume fraction of the double kink $(=\frac{\pi r^2 z}{V})$ where V is the volume of the polymer. The energy is then approximated as $W = \frac{\pi r^2 z}{V}(1 - \cos(\omega))\sigma_{zz} V \approx \pi r^2 z \omega^2 \frac{\sigma_{zz}}{2}$ for $\omega < 1$. Comparing with Eq. (2), the stress τ in the last term of Eq. (2) is the maximum shear stress during uniaxial compression $\tau = \frac{\sigma_{zz}}{2}$.

[1] A wedge disclination loop involves a wedge-like cut at one side of the cross section and insertion of the wedge on the other side of the cut as shown in Fig. 8(b).

Please cite this article in press as: Sundararaghavan, V., Kumar, A. Molecular dynamics simulations of compressive yielding in cross-linked epoxies in the context of Argon theory. Int. J. Plasticity (2013), http://dx.doi.org/10.1016/j.ijplas.2013.01.004

For the kinking to nucleate under an applied load, a critical configuration with length z and angle ω can be identified that maximizes ΔG. Argon argued that angle ω coordinate is related to intra-molecular energies while yielding is primarily governed by the inter-molecular energies, described by z coordinate. Thus, the saddle-point was obtained by differentiating the free enthalpy only with respect to z while keeping ω constant. It is found that the maxima of ΔG is obtained when:

$$\frac{z}{r} = \left(\frac{45}{8(1-\nu)}\frac{\mu}{\tau}\right)^{1/6} \tag{3}$$

The critical free enthalpy corresponding to this configuration is (substituting $\frac{z}{r}$ from Eq. (3) in Eq. (2)):

$$\Delta G^* = \frac{3\pi\mu\omega^2 r^3}{16(1-\nu)}\left[1 - 8.5(1-\nu)^{5/6}\left(\frac{\tau}{\mu}\right)^{5/6}\right] \tag{4}$$

Substituting the expression of ΔG^* in the Arrhenius form (Eq. (1)) and and rewriting terms, the critical stress is obtained as:

$$\tau = \frac{0.077}{1-\nu}\mu\left[1 - \frac{16(1-\nu)kT}{3\pi\mu\omega^2 r^3}\ln(\dot{\gamma}_o/\dot{\gamma})\right]^{6/5} \tag{5}$$

Argon theory presents a compelling molecular mechanism for yielding in epoxy resins and has been verified experimentally in the past but so far no comparisons have been made using molecular dynamics. The critical ratio $\frac{z}{r}$ was computed by using Poisson's ratio, yield stress and shear modulus data obtained from molecular dynamics simulations (shown in Fig. 6 and Fig. 7) in Eq. (3). The variation of $\frac{z}{r}$ with temperature is plotted in Fig. 9 and the results show only a weak dependence on temperature. This is because the ratio σ_{zz}/μ is practically unchanged with temperature as illustrated in Fig. 10(a). Since activation of kinks is related to yielding, the yield strain is also expected to have a weak sensitivity to temperature changes. Molecular dynamics data is used to illustrate the relationship between yield strain and temperature in Fig. 10(b). In addition, at T = 0 K, Eq. (5) also indicates that the yield strain approximated as $\frac{\tau}{\mu} = \frac{0.077}{1-\nu}$ does not show a strong dependence on strain rate. These ideas motivate the application of 'strain-invariant' failure theories of Gosse and Christensen (2001) that relates the failure point with a critical strain measure (either dilatational or deviatoric) rather than a critical stress measure.

We performed molecular simulations at a low temperature of 1 K to suppress thermal oscillations and allow measurement of critical quantities (z, ω) more accurately. Simulations were performed at a strain rate of 10^{10} s^{-1} up to a compressive strain of 20% along x- direction. Molecular trajectories from LAMMPS was transferred to Materials Studio software for visualization. It is observed that kinking (or wedge disclinations) indeed occurs as proposed by Argon (as shown in Fig. 11). It is seen that yielding proceeds through several localized kinking processes. The location of the first steep drop in stress value in the stress-strain curve (shown in Fig. 7(a)) is related to initiation of the first molecular kink (as observed by careful visualization of all 107 monomeric subunits). As deformation proceeds beyond this point, the stress initially increases until another chain starts to kink, a second steep drop in stress is seen and then the process repeats again. At the continuum level, the kinking of several millions of polymer chains are cumulatively expected at the critical strain value and the yielding transition macroscopically appears to be smooth. In this context, we refer to MD simulations of amorphous polymers (work

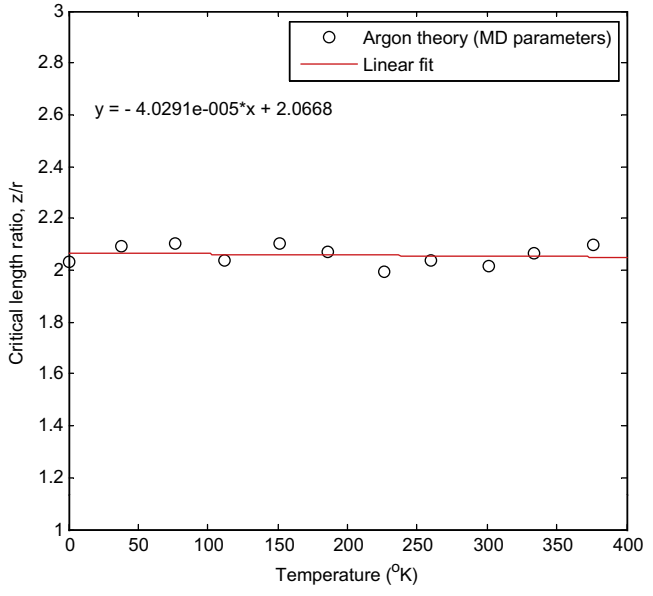

Fig. 9. Variation of kink segment length (z) with temperature using data from MD simulations in Argon theory.

Please cite this article in press as: Sundararaghavan, V., Kumar, A. Molecular dynamics simulations of compressive yielding in cross-linked epoxies in the context of Argon theory. Int. J. Plasticity (2013), http://dx.doi.org/10.1016/j.ijplas.2013.01.004

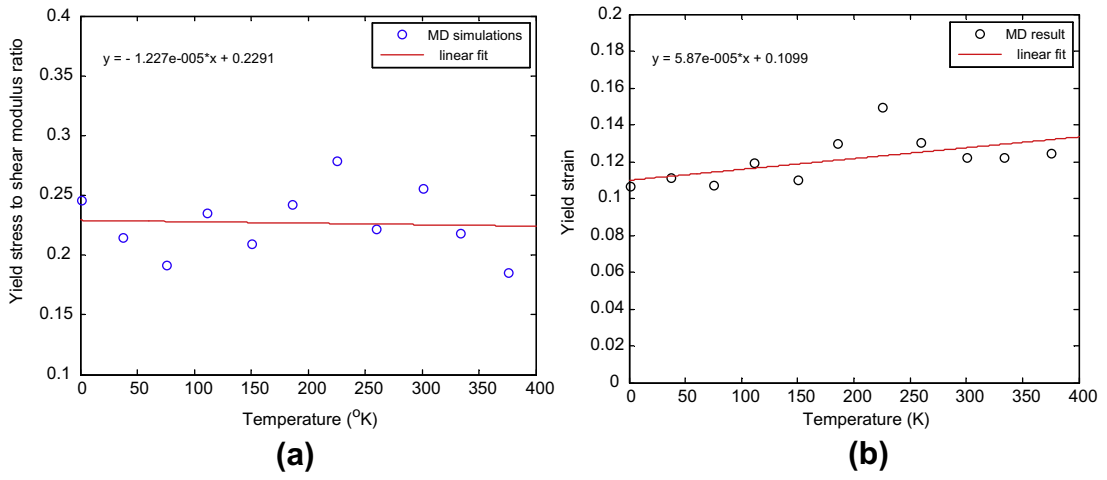

Fig. 10. (a) Ratio of yield stress and shear modulus as a function of temperature (b) Yield strain as a function of temperature (from molecular dynamics data).

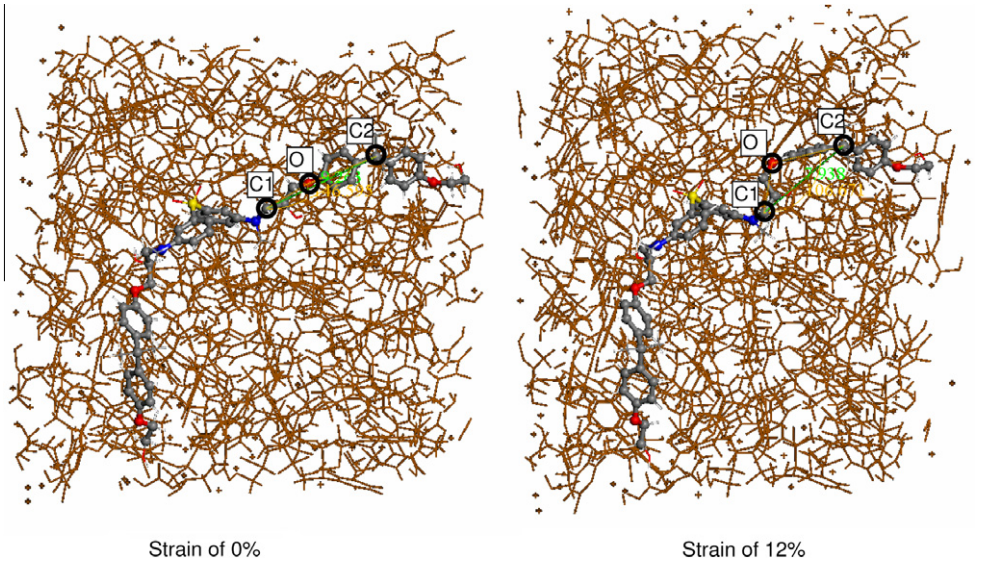

Fig. 11. Visualization of the kinking process in a representative chain. The chain configuration at a strain of 12% involves a double kink.

of Argon et al. (1992) and references therein) where similar stress drop events were noted. These stress drop events were unambiguously identified as irreversible unit plastic relaxations since unloading did not reverse the drop in stresses. These simulations were carried out using a single packed polymer chain in which cooperative motion of several chains was seen. In the present simulation, however, such cooperative flow is restricted due to the presence of cross-links and the deformation mechanism is seen to be more localized.

The deformation mechanism corresponding to the first steep drop was isolated and visualized (in more detail) as a function of strain in Fig. 12. Here, carbon atoms are colored grey, oxygen is colored red,[2] nitrogen is colored blue, sulfur is colored yellow while hydrogen atoms are not illustrated. The epoxy monomer is seen to undergo a kinking process that initiates at a strain of 10% and a stabilized kink configuration is seen at a strain of 12%. There is little change in the kink configuration after this strain level is reached.

In theory described above, the kinking segment is approximated an elastic cylinder of radius r. From the molecular simulation at 1 K, the radius of the chain undergoing kinking was found by measuring the distances of atoms in the kinking segment to the closest atoms in adjacent chains and an average radius of $r = 3.93A$ was calculated. Taking into account the

[2] For interpretation of color in Fig. 13, the reader is referred to the web version of this article.

Please cite this article in press as: Sundararaghavan, V., Kumar, A. Molecular dynamics simulations of compressive yielding in cross-linked epoxies in the context of Argon theory. Int. J. Plasticity (2013), http://dx.doi.org/10.1016/j.ijplas.2013.01.004

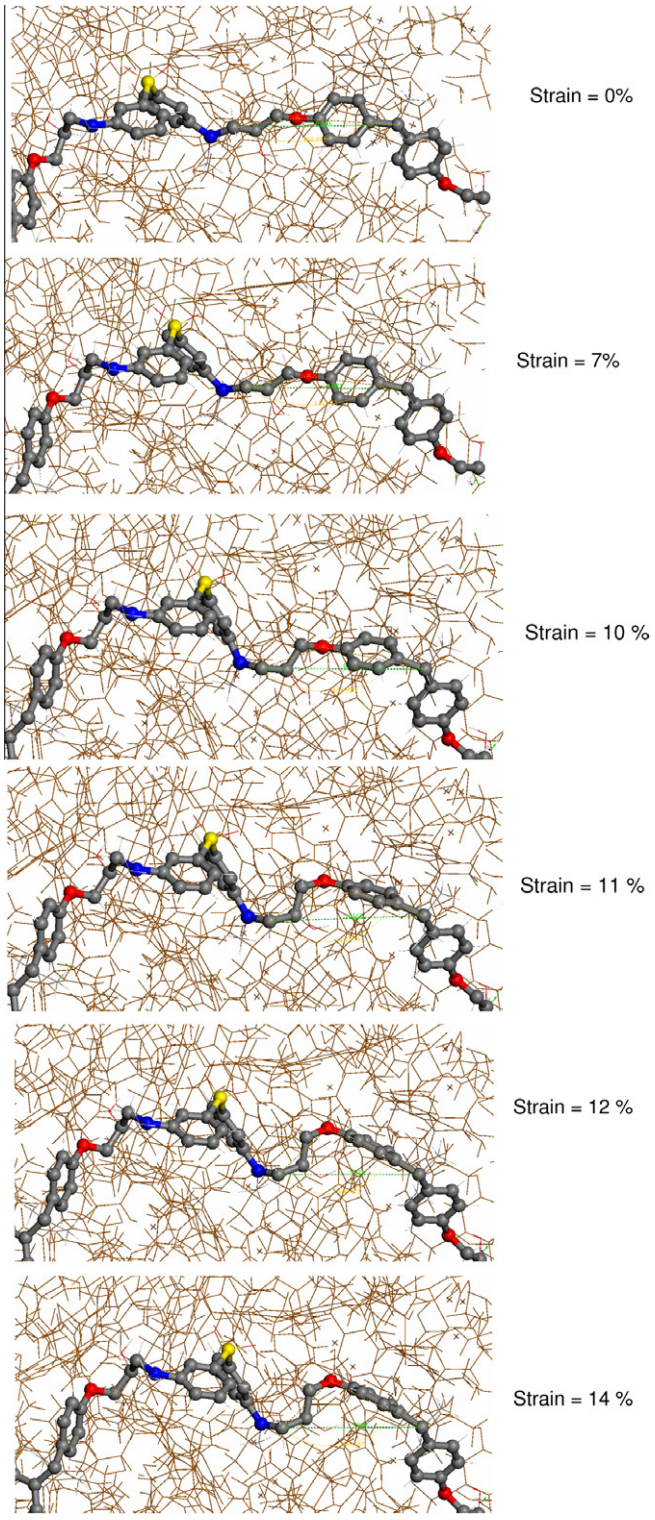

Fig. 12. Visualization of the kinking process in a representative chain in more detail as a function of strain. The key parameters (z and apex angle) in the kinking chain are also indicated in each snapshot.

thermal expansion ($\alpha = 55 \times 10^{-6}$/K), the radius is expected to increase with temperature as $r = 3.93(1 + \alpha\Delta T)$ to a value of 4.0 Å at 300 K. This compares well with the molecular radius found in Ref. Lee (1988) in the range of 4.10–4.69 Å through calibration with experimental stress–strain curves at quasi-static loading rates.

Please cite this article in press as: Sundararaghavan, V., Kumar, A. Molecular dynamics simulations of compressive yielding in cross-linked epoxies in the context of Argon theory. Int. J. Plasticity (2013), http://dx.doi.org/10.1016/j.ijplas.2013.01.004

Bond torsion analysis was performed to identify the centers of rotation of the wedge disclination. The torsion angles for various bonds in the epoxy chain were computed as a function of strain and are plotted in Fig. 13(b). Bonds '4' and '11' are seen to undergo large rotations compared to other atoms to the left and right respectively. For example, C-C bond '12' shows a 14 degrees rotation followed by a -75.5° rotation of the C–C bond '11'. Similarly, it is seen that the C–N bond '3' undergoes a rotation -38°, while the C–C bond '4' shows a large rotation of $+83.83^\circ$ at the same strain level. Based on these observations, the center of rotations were fixed on carbon atoms (named C1 and C2) attached to bonds undergoing significant rotations, namely (3,4) and (11,12) in Fig. 13(a). The kink angle ω was measured from the initial (16^o at 0% strain) and final (52.78° at 12% strain) values of bond angle between atoms C3, C1 and C2 atoms giving a kink angle of $\omega = 36.78^\circ$ (shown in Fig. 13(a)). From the stress–strain response shown in Fig. 13(c), the critical strain at which the steep drop in stress occurs is measured to be about 11%. A large jump in the distance between $C1$ and $C2$ atoms is also seen to occur at 11% strain corresponding to a kink distance of $z = 8.365$ Å. From Fig. 13(c), the maximum torsion angle for the bonds attached to $C1$ and $C2$ is seen to occur at 12% strain corresponding to a C1-C2 distance of $z = 7.938$ Å (C1-C2 distances are shown in Fig. 12). The critical length calculated from Argon theory (by using the elastic modulus and yield stress computed from molecular simulation in Eq. (3)) is $z = 7.984$ Å at $T = 1$ K which is close to that seen in the MD simulations. Also, it is seen that the Argon theory prediction is close to a linear fit for this data (although Eq. (5) indicates a 6/5 power law).

The activation process for the kinking defect can be considered to be of the form shown in Fig. 14. When a strain γ is applied to a sample, the system will achieve a new position of stable equilibrium S where the local slope, $\frac{1}{V}\partial\Delta F/\partial\sigma$, is equal to the applied strain γ. If the system can be supplied with a energy fluctuation ΔG_f (supplying an extra stress $\Delta\sigma_f$) it will reach

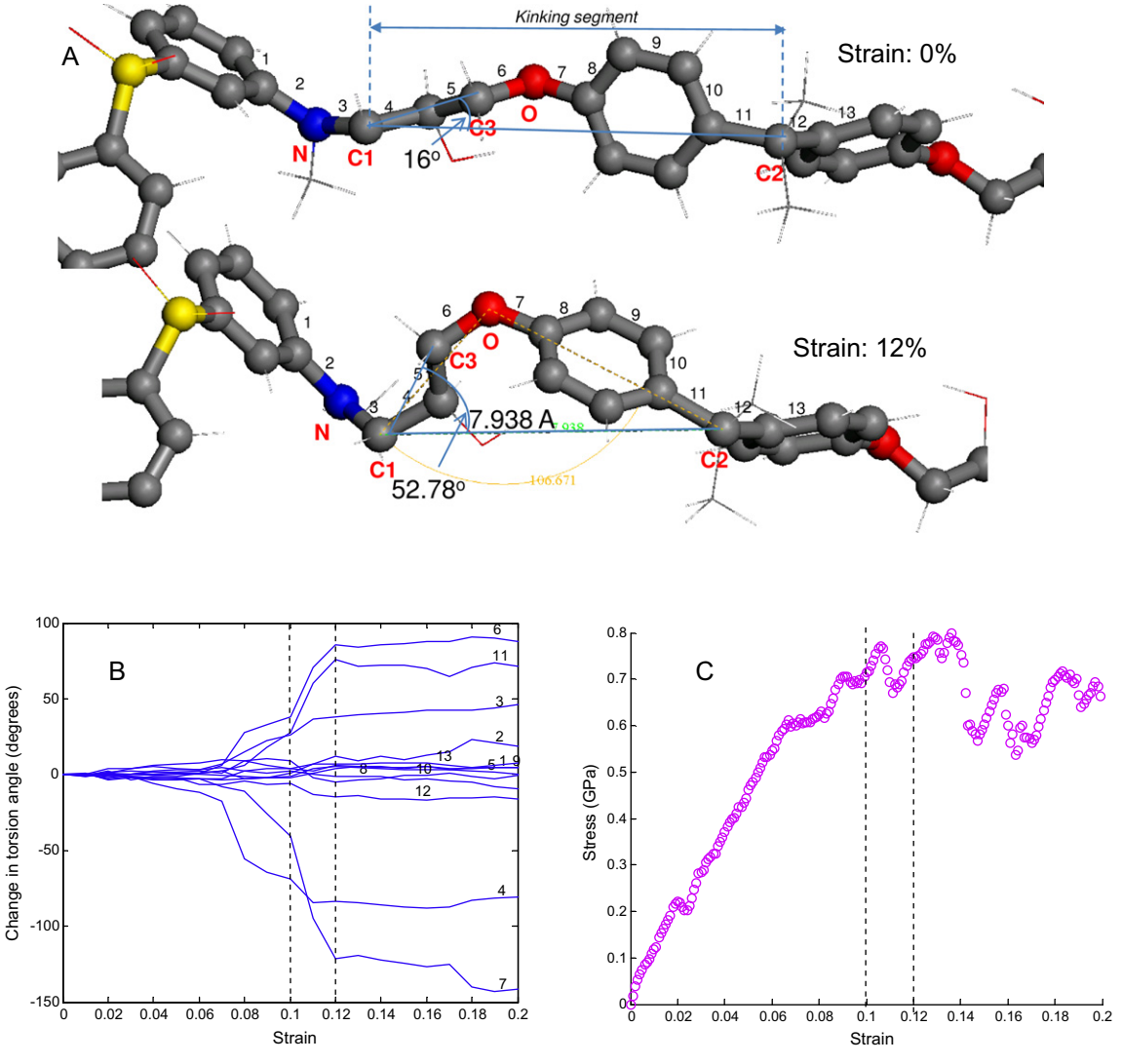

Fig. 13. (A) The initial and final configuration of a segment of a chain that undergoes kinking; (B) Change in torsion angles of bonds numbered in (A) as a function of strain; (C) The strain window over which large changes in torsion angles is seen.

Please cite this article in press as: Sundararaghavan, V., Kumar, A. Molecular dynamics simulations of compressive yielding in cross-linked epoxies in the context of Argon theory. Int. J. Plasticity (2013), http://dx.doi.org/10.1016/j.ijplas.2013.01.004

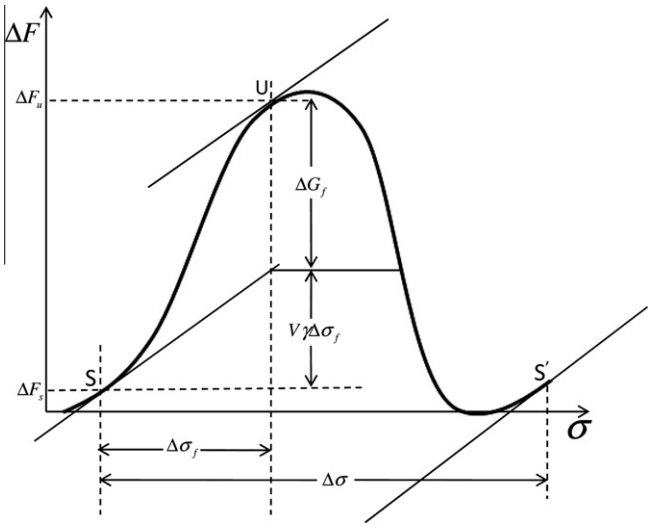

Fig. 14. Helmholtz free energy versus stress showing the initial state (S), the intermediate state (U) (a result of a stress fluctuation $\Delta\sigma_f$), and the final stable state S' with a large stress change $\Delta\sigma$.

another point U on the contour with the same slope (strain) where the system is in unstable equilibrium. Any further increase in stress will relax the system to a new stable equilibrium configuration given by S'. This final configuration has the same strain level but the system has a much lower stress with a stress decrement of $\Delta\sigma$ as seen in the stress–strain curves shown previously. The activation energy ΔG^* for this process can be inferred from Fig. 14 as:

$$\Delta G^* = (\Delta F_u - \Delta F_s) - \Delta\sigma_f \gamma V \tag{6}$$

We carried out a nudged elastic band (NEB) calculation of the kinking segment to compute the energy barrier. NEB was used to find the height of the energy barrier associated with the kinking process. An initial kink state and a final kink state were taken at a strain level of 10.61% and 11.11% respectively from the results of the MD calculation shown in Fig. 13(c). A set of 11 replicas between the initial and final kink states were created through interpolation of atomic coordinates. In a NEB calculation, each atom in a replica is connected to the same atom in adjacent replicas by springs, which induce inter-replica forces. NEB was performed in two stages. In the first stage of NEB, the set of replicas are allowed to converge toward the minimum energy path (MEP) of conformational states that transition over the barrier. In the second stage of NEB, the replica with the highest energy is selected and the inter-replica forces on it are converted to a force that drives its atom coordinates to the top or saddle point of the barrier, via the barrier-climbing calculation described in Henkelman et al. (2000) and implemented in LAMMPS package. The segment of the molecule between atoms marked $C1$ and $C2$ in Fig. 13(a) is taken to be kinking segment. The atoms around this critical segment are not connected by springs across replicas, and only provide a background force field during the NEB procedure. When both stages are complete, the potential energies for the set of replicas represents the energy profile of the barrier along the MEP.

Fig. 15 shows the energy profile for the critical segment plotted with potential energy in the y-axis and the normalized reaction coordinate in the x-axis. The reaction coordinate for each replica is the norm of distances between its atoms and the preceding replica's atoms, added to the reaction coordinate of the preceding replica. The x-axis denotes the value after normalizing with the reaction coordinate of the final replica. At 1 K, the change in potential energy will be approximately equal to mechanically induced energy increment $\Delta\sigma_f \gamma V$ due to negligible thermal fluctuation. Using the energetics from the NEB calculation, it is possible to predict the jump in stresses during activation of the kink at low temperatures:

$$\Delta\sigma_f = \frac{(\Delta F_u - \Delta F_s)}{\gamma V} \tag{7}$$

The critical change in potential energy (energy difference between reaction coordinate 0.3 and 0.4) is observed to be 2.49E−19 J from Fig. 15. Using the volume of the unit cell a^3 with $a = 38$ Å) and the strain ($\gamma = 0.1091$) around which the drop in stress is seen, the corresponding change in stress can be predicted using Eq. (7). The value found based on this approach was 41.7 MPa which is within the observed drop of 42.5 MPa seen from the stress–strain curve in Fig. 13(c).

Argon theory excludes twist disclinations (torsions) in the analysis of critical energy. Although bond torsions have been proposed as mechanisms for yielding in non-cross-liked systems such as polyethylene using MD simulations (in tensile mode simulation of Yashiro et al. (2003)), kink mechanism (Argon theory) is seen to agree well with experimentally observed compressive yield strengths of several cross-linked systems (Lee, 1988). A visualization of atomic trajectories during compression of epoxy shows continuous torsion of several segments of epoxy molecule during deformation even before the sud-

Please cite this article in press as: Sundararaghavan, V., Kumar, A. Molecular dynamics simulations of compressive yielding in cross-linked epoxies in the context of Argon theory. Int. J. Plasticity (2013), http://dx.doi.org/10.1016/j.ijplas.2013.01.004

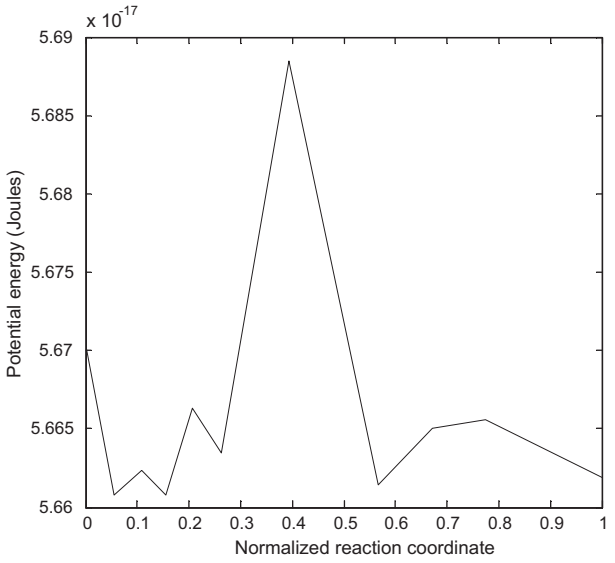

Fig. 15. Change in energy as a function of reaction coordinate for the kinking segment as obtained from the nudged elastic band calculation.

den drop in stresses in seen. In order to better present the effect of torsion, we have provided in Fig. 16 a plot of energy contribution from bond torsions as computed during the MD simulation in Fig. 13(c). Here, it is seen that torsional energies continuously increase during loading, even within the linear portion of the stress strain response. In addition, there are no significant changes in bond torsion energies in the strain window within which the critical drop in stresses was observed. Although, it is obvious that bond torsions are indeed a source of plastic deformation (Yashiro et al., 2003), the sudden large drop in stresses seen in the stress strain curve cannot be predicted from the observed torsion energy changes. Nudged elastic band approach describes the stress drop quite well from the point of view of the energetics of the kink mechanism. Further, the observed value of critical segment length is in close agreement with Argon theory which is based on kink disclination mechanism. In addition, Argon theory provides good agreement with experimentally observed yield strength in several epoxy systems (Lee, 1988). These observations indicate that kink mechanism is indeed the reason behind the large drop in stresses seen in the MD simulations.

While Argon theory has been successfully compared with experiments using fitted parameters in many previous works (Lee, 1988; Yamini and Young, 1980; Cook et al., 1998), this is the first attempt at measuring these parameters quantitatively from MD simulations. We used these parameters to calculate the relationship between yield stress and temperature pre-

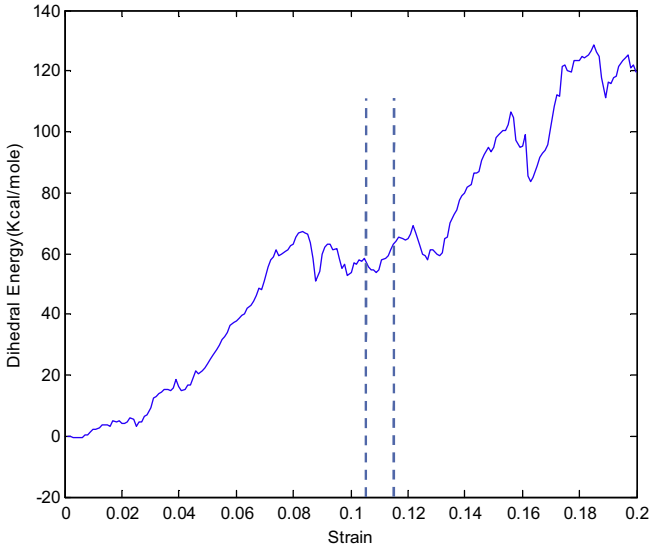

Fig. 16. Change in dihedral energy as a function of strain. The strain window within which the large drop in stress is seen is indicated as a dotted line.

Please cite this article in press as: Sundararaghavan, V., Kumar, A. Molecular dynamics simulations of compressive yielding in cross-linked epoxies in the context of Argon theory. Int. J. Plasticity (2013), http://dx.doi.org/10.1016/j.ijplas.2013.01.004

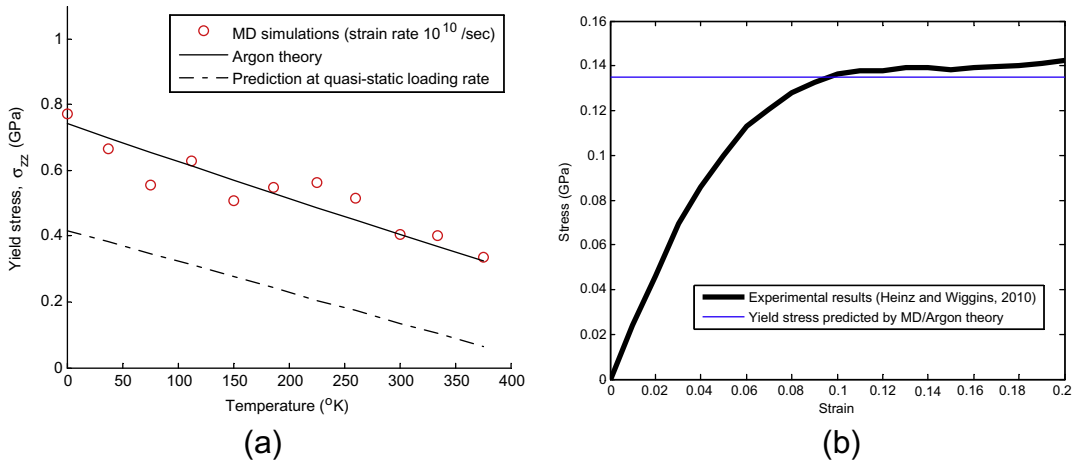

Fig. 17. (a) The yield stress versus temperature curve predicted by molecular dynamics simulations is compared with Argon theory. The expected response at quasi-static rates are also shown which indicate at yield stress of 0.134 GPa at 300 K. (b) Experimental results from Heinz and Wiggins at quasi-static loading rates and room temperature indicate a yield stress of 0.138 GPa at 11% strain.

dicted by Argon theory. The elastic properties (Poisson's ratio and elastic modulus at $T = 1$ K) are taken from Fig. 6 and used in Eq. (5) to extract the yield stresses. The Argon theory prediction shown in Fig. 17 show good correlation with yield stresses computed from MD calculations.

While this work demonstrates the approach to identify geometrical parameters at high strain rates, it is computationally difficult to extract these values in quasi-static regimes. At small strain rates, the molecules have sufficient time to rearrange and relax which changes the kink and torsion angles to a value different from those measured at high strain rates. However, experiments in Ref. Behzadi and Jones (2005) reveal that the slope of yield stress versus temperature curve in epoxy resins is approximately the same at different strain rates. The slope obtained from MD simulations at a high strain rate is -9.417×10^{-4} GPa /K as seen from Fig. 7(b). If the slope were unchanged at quasi-static rates, the yield stress is expected to approximately follow a linear fit $\sigma_{zz} = \sigma_{zz}^{\circ} - 9.417 \times 10^{-4}\, T$ where σ_{zz}° is the yield stress at quasi-static rate and $T = 0$ K. Argon theory provides an avenue for extracting the value of σ_{zz}° using data from molecular statics simulation. The elastic modulus and Poisson's ratio from molecular statics results were $E = 4.83$ GPa and $\nu = 0.33$ (Fig. 5), using which Argon theory gives a theoretical yield stress of $\sigma_{zz}^{o} = 2\frac{0.077}{1-\nu}\mu = 0.4174$ GPa. The procedure results in a prediction of 0.135 GPa yield stress at quasi-static rates and room temperature ($T = 300$ K). This is very close to the experimental yield stress of 0.138 GPa reported in recent experiments (Heinz and Wiggins, 2010) (with loading rate of 8.33×10^{-4} s^{-1}) as shown in Fig. 17(b). The steps needed for extraction of yield stresses under quasi static loading conditions from high strain rate MD simulations in the context of Argon theory is summarized here: (i) A linear fit for yield stress versus temperature is computed from the high rate MD simulation and the slope is computed (which is same as the slope at quasi-static rates based on experiments in Ref. Behzadi and Jones (2005)). (ii) Using Argon Theory (Eq. (5)) and and elastic properties from molecular statics simulation, the intercept (yield stress at 0 K) is estimated. (iii) The yield stress at different temperatures can be extracted through a linear fit based on the slope and intercept computed from steps (i) and (ii) respectively. The ability to predict quasi-static behavior at non-zero temperatures using Argon theory and MD simulations is especially attractive in the context of performing computational materials design even before synthesis of the polymer.

We emphasize that double kink mechanism can be clearly identified from MD simulations only at low temperatures (1 K) when thermal motions are absent. As shown in Fig. 7(a), the plastic response is smoother at higher temperature without much of the sharp stress drop as a result of thermal penetration of activation energy barriers. At higher temperatures, the stress drop occurs over a larger range of strains over which multiple mechanisms including kinking, twisting of chains and localized shear may become active. Thus, further study is needed to clarify the role of the kink mechanism (Argon theory) at moderate temperatures and high strain rates.

4. Conclusions

Plastic deformation in DGEBA/DDS cross-linked epoxy in low temperature glassy state has been studied using molecular dynamics simulations. The molecular model was built using the dendrimer approach and a representative epoxy structure was built by subjecting the structure to several thermal annealing cycles. The optimized epoxy structure successfully reproduced the experimental dilatometric curves reported in literature. Subsequently, realistic compression tests were performed under periodic boundary conditions to understand the molecular mechanisms of yielding in cross-linked epoxies. At low temperatures, a steep drop in stresses at the yield point was attributed to the activation of a wedge disclination (kinking) in the epoxy chain. For the first time in literature, both the chemistry and geometry (critical length, angles, bond torsions)

Please cite this article in press as: Sundararaghavan, V., Kumar, A. Molecular dynamics simulations of compressive yielding in cross-linked epoxies in the context of Argon theory. Int. J. Plasticity (2013), http://dx.doi.org/10.1016/j.ijplas.2013.01.004

of the critical segment that undergoes the kinking process have been measured. Argon theory, which is based on an elastic model of a wedge disclination, gives a critical kinking segment length that agrees well with molecular simulations. The yield stress versus temperature predictions of Argon theory were directly compared with molecular simulation results and show good correlation. Argon theory is investigated as an option for extracting mechanical response at quasi-static strain rates from high strain rate molecular simulations. By combining the theoretical yield stress at $T = 0$ K predicted by Argon theory and the slope of yield stress versus temperature seen from high rate molecular simulations, an yield stress of 0.135 GPa is estimated at 300 K and quasi-static loading rate. The result is very close to the experimental yield stress of 0.138 GPa reported in recent experiments (Heinz and Wiggins, 2010). The results indicate tremendous promise of molecular simulations for the purpose of computing engineering properties and for future development of rigorous, physically-based constitutive models (Anand et al., 2009; Ames et al., 2009) for epoxies. The approach will be extended towards study of emerging nanocomposites where defect mechanisms such as disclinations may be modified or affected by the presence of nano-reinforcements such as functionalized nanotubes (Yang et al., 2013).

Acknowledgements

The work presented here was supported by Boeing Company (Seattle, WA). The authors would like to acknowledge Dr. Steve Christensen and Dr. Andrea Browning, Boeing Research and Technology for their assistance in this work. The authors acknowledge the support of the University of Michigan Center for Advanced Computing (CAC), a high-performance computing center located in the Ann Arbor campus.

References

Accelrys Software Inc., 2007. Discovery Studio Modeling Environment: Release 5.5, San Diego.
Ames, N.M., Srivastava, V., Chester, S.A., Anand, L., 2009. A thermo-mechanically coupled theory for large deformations of amorphous polymers. Part II: Applications. Int. J. Plasticity 25 (8), 1495–1539.
Anand, L., Ames, N.M., Srivastava, V., Chester, S.A., 2009. A thermo-mechanically coupled theory for large deformations of amorphous polymers. Part I: Formulation. Int. J. Plasticity 25 (8), 1474–1494.
Argon, A.S., 1973. A theory for the low-temperature plastic deformation of glassy polymers. Philos. Mag. 28, 839–865.
Argon, A.S., 1975. Plastic deformation in glassy polymers. In: Polymeric Materials. A.S.M., Metals Park, Ohio, pp. 411–486.
Argon, A.S., Bessonov, M.I., 1977. Plastic flow in glassy polymers. Polym. Eng. Sci. 17 (3), 174–182.
Argon, A.S., Mott, P.H., Suter, U.W., 1992. Simulation of plastic deformation in a flexible chain glassy polymer. Phys. Stat. Sol. (b) 172, 193–204.
Behzadi, S., Jones, F.R., 2005. Yielding behavior of model epoxy matrices for fiber reinforced composites: effect of strain rate and temperature. J. Macromol. Sci. Part B 44 (6), 993–1005.
Bowden, P.B., Raha, S., 1974. A molecular model for yield and flow in amorphous glassy polymers making use of a dislocation analogue. Philos. Mag. 29 (1), 149–166.
Christensen, S., 2007. Atomistically explicit molecular dynamics simulations of thermosetting polymers. In: Proc. of 39th ISTC SAMPE Conf., 2007.
Cook, W.D., Mayr, A.E., Edward, G.H., 1998. Yielding behavior in model epoxy thermosets - II. Temperature dependence. Polymer 39 (16), 3725–3733.
Dauber-Osguthorpe, P., Roberts, V.A., Osguthorpe, D.J., Wolff, J., Genest, M., Hagler, A.T., 1988. Structure and energetics of ligand binding to proteins: E. coli dihydrofolate reductase-trimethoprim, a drug-receptor system. Proteins: Struct. Funct. Genet. 4, 31–47.
Eyring, H., 1936. Viscosity, plasticity, and diffusion as examples of absolute reaction rates. J. Chem. Phys 4, 283–291.
Frenkel, D., Smit, B., 2002. Understanding molecular simulation: from algorithms to applications. Academic Press, San Diego.
Gilman, J.J., 1968. The plastic response of solids. In: Rosenfield, A.R. (Ed.), Dislocation Dynamics. McGraw-Hill, New York, p. 3.
Gosse, J.H., Christensen, S., 2001. Strain invariant failure criteria for polymers in composite materials, American Institute of Aeronautics and Astronautics, AIAA-2001–1184.
Heine, D.R., Grest, G.S., Lorenz, C.D., Tsige, M., Stevens, M.J., 2004. Atomistic simulations of end-linked poly(dimethylsiloxane) networks: structure and relaxation. Macromolecules 37, 3857–3864.
Heinz, S.R., Wiggins, J.S., 2010. Uniaxial compression analysis of glassy polymer networks using digital image correlation. Polym. Test. 29, 925–932.
Henkelman, G., Uberuaga, B.P., Jónsson, H., 2000. A climbing image nudged elastic band method for finding saddle points and minimum energy paths. J. Chem. Phys. 113, 9901–9904.
Jaramillo, E., Wilson, N., Christensen, S., Gosse, J., Strachan, A., 2012. Energy-based yield criterion for PMMA from large-scale molecular dynamics simulations. Phys. Rev. B 85 (2), 1–7, 024114.
Kang, K., Cai, W., 2010. Size and temperature effects on the fracture mechanisms of silicon nanowires: molecular dynamics simulations. Int. J. Plasticity 26 (9), 1387–1401.
Knox, C.K., Andzelm, J.W., Lenhart, J.L., Browning, A.R., Christensen, S., 2010. High strain rate mechanical behavior of epoxy networks from molecular dynamics simulations. In: 27th Army Science Conference Proceedings, 2010.
Lee, S.M., 1988. Plastic deformation in epoxy resins. In: Dickie, R. et al. (Eds.), Cross-Linked Polymers, ACS Symposium series. American Chemical Society, Washington, DC, pp. 136–144 (Chapter 11).
Li, J.C.M., Gilman, J.J., 1970. Disclination loops in polymers. J. Appl. Phys. 41 (11), 4248–4256.
Plimpton, S., 1995. Fast parallel algorithms for short-range molecular dynamics. J. Comput. Phys. 117, 1–19.
Robertson, R.E., 1966. Theory for the plasticity of glassy polymers. J. Chem. Phys. 44, 3950–3957.
Rottach, D.R., Curro, J.G., Budzien, J., Grest, G.S., Svaneborg, C., Everaers, R., 2007. Molecular dynamics simulations of polymer networks undergoing sequential cross-linking and scission reactions. Macromolecules 40, 131–139.
Spearot, D.E., Jacob, K.I., McDowell, D.L., 2007. Dislocation nucleation from bicrystal interfaces with dissociated structure. Int. J. Plasticity 23 (1), 143–160.
Stachurski, Z.H., 1997. Deformation mechanisms and yield strength in amorphous polymers. Prog. Polym. Sci. 22, 407–474.
Tcharkhtchi, A., Gouin, E., Verdu, J., 2000. Thermal expansion of epoxide amine networks in the glassy state. J. Polym. Sci. Part B: Polym. Phys. 38, 537–543.
Theodorou, D.N., Suter, U.W., 1986. Atomistic modeling of mechanical properties of polymeric glasses. Macromolecules 19, 139–154.
Varshney, V., Patnaik, S.S., Roy, A.K., Farmer, B.L., 2008. A molecular dynamics study of epoxy-based networks: cross-linking procedure and prediction of molecular and material properties. Macromolecules 41, 6837–6842.
Wang, Q., Storm, B.K., Houmoller, L.P., 2003. Study of the isothermal curing of an epoxy prepreg by near-infrared spectroscopy. J. Appl. Polym. Sci. 87, 2295–2305.
Weinberger, C.R., 2011. The structure and energetics of and the plasticity caused by Eshelby dislocations. Int. J. Plasticity 27 (9), 1391–1408.
Wu, C., Xu, W., 2006. Atomistic molecular modelling of crosslinked epoxy resin. Polymer 47, 6004–6009.

Please cite this article in press as: Sundararaghavan, V., Kumar, A. Molecular dynamics simulations of compressive yielding in cross-linked epoxies in the context of Argon theory. Int. J. Plasticity (2013), http://dx.doi.org/10.1016/j.ijplas.2013.01.004

Xu, S., Guo, Y.F., Ngan, A.H.W., in press. A molecular dynamics study on the orientation, size, and dislocation confinement effects on the plastic deformation of Al nanopillars. Int. J. Plasticity. http://dx.doi.org/10.1016/j.ijplas.2012.11.002.

Yamini, S., Young, R.J., 1980. The mechanical properties of epoxy resins Part 1 Mechanisms of plastic deformation. J. Mat. Sci. 15, 1814–1822.

Yang, S., Yu, S., Ryu, J., Cho, J.-M., Kyoung, W., Han, D.-S., Cho, M., 2013. Nonlinear multiscale modeling approach to characterize elastoplastic behavior of CNT/polymer nanocomposites considering the interphase and interfacial imperfection. Int. J. Plasticity 41, 124–146.

Yarovsky, I., Evans, E., 2002. Computer simulation of structure and properties of crosslinked polymers: application to epoxy resins. Polymer 43, 963–969.

Yashiro, K., Ito, T., Tomita, Y., 2003. Molecular dynamics simulation of deformation behavior in amorphous polymer: nucleation of chain entanglements and network structure under uniaxial tension. Int. J. Mech. Sci. 45, 1863–1876.

Please cite this article in press as: Sundararaghavan, V., Kumar, A. Molecular dynamics simulations of compressive yielding in cross-linked epoxies in the context of Argon theory. Int. J. Plasticity (2013), http://dx.doi.org/10.1016/j.ijplas.2013.01.004